
# Proceedings of the Third International Workshop on Sustainable Ultrascale Computing Systems (NESUS 2016) Sofia, Bulgaria

Jesus Carretero, Javier Garcia Blas, Svetozar Margenov
(Editors)

October, 6-7, 2016

Blaheta, R., Georgiev, I., Georgiev, K., Jakl, O., Kohut, R., Margenov, S. & Starý, J. (2016). Analysis of fiber-reinforced concrete: micromechanics, parameter identification, fast solvers. En *Proceedings of the Third International Workshop on Sustainable Ultrascale Computing Systems (NESUS 2016) Sofia, Bulgaria* (pp. 31-36). Madrid: Universidad Carlos III de Madrid. Computer Architecture, Communications, and Systems Group (ARCOS).

# Analysis of fiber-reinforced concrete: micromechanics, parameter identification, fast solvers

R. Blaheta[a], I. Georgiev[b], K. Georgiev[b], O. Jakl[a], R. Kohut[a], S. Margenov[b], J. Starý[a]

[a] Institute of Geonics, Czech Academy of Sciences, Ostrava, CR
[b] Institute of Information and Communication Technologies, Bulgarian Academy of Sciences, Sofia, BG
[blaheta, jakl, kohut, stary]@ugn.cas.cz, [ivan.georgiev, georgiev, margenov]@parallel.bas.bg

**Abstract**

*Ultrascale computing is required for many important applications in chemistry, computational fluid dynamics etc., see an overview in the paper Applications for Ultrascale Computing by M. Mihajlovic et al. published in the International Journal Supercomputing Frontiers and Innovations, Vol 2 (2015). In this abstract we shortly describe an application that involves many aspects described in the above paper - the multiscale material design problem. The problem of interest is analysis of the fiber reinforced concrete and we focus on modelling of stiffness through numerical homogenization and computing local material properties by inverse analysis. Both problems require a repeated solution of large-scale finite element problems up to 200 million degrees of freedom and therefore the importance of HPC and ultrascale computing is evident.*

***Keywords*** Analysis of fiber-reinforced concrete, homogenization, identification of parameters, parallelizable solver, additive Schwarz method, two-level parallelization

## I. Introduction

This paper is a continuation of paper [1] presented at the NESUS workshop in Cracow, Poland 2015. While [1] focused on linear micromechanics exploiting CT scans for determination of microstructure and numerical homogenization, this paper is driven by a specific application - analysis of fiber-reinforced concrete. This analysis includes an identification problem and stochastic uncertainty, which brings new dimension and enhances the need for fast solvers and ultrascale computations.

Fiber-reinforced concrete with steel fibers has a lot of applications in civil and geotechnical engineering. It is less expensive than hand-tied rebar, while still increasing the tensile strength many times. The shape, dimension, and length (standard 1 mm diameter, 45 mm length) of the fiber together with fiber volume amount and distribution are important parameters influencing the tensile strength of concrete.

The analysis includes assessment of tensile stiffness for several samples of fiber-reinforced concrete which differ in amount and distribution of fibers. These samples are scanned by CT and analysed with provided elastic parameters for steel fibers and concrete matrix. The detailed scan of a sample leads to solving of elastic problems with about 200 million degrees of freedom.

As the global response of the samples can be tested on a loading frame, then the output allows to solve an inverse identification procedure to determine the elastic properties of the concrete matrix. In this way we can both determine the properties of concrete matrix, which can also be variable to some extent, as well as assess whether some discrepancy can be explained by imperfect bonding of fibers.

It is also possible not only to investigate selected physical samples of the fiber-reinforced concrete but to do stochastic analysis with a repeated generation of stochastic microstructure, see e.g. [5, 6].

## II. Homogenization and identification of parameters

The numerical homogenization starts with solving the elasticity problem on the domain $\Omega$ with given microstructure. The solution is possibly repeated for different loadings by imposed boundary conditions. In an abstract way, we denote the loading conditions by $L$ or in the case of multiple loading by $L^{(k)}$. The stress and strain tensors $\sigma^{(k)}$ and $\varepsilon^{(k)}$ are averaged over $\Omega$ and the homogenized elasticity tensor $\bar{C} \in R^{6\times6\times6\times6}_{sym}$, $C = \left[c_{ijkl}\right]$, $c_{ijkl} = c_{jikl} = c_{klij}$ is determined

as a (generalized) solution of the system

$$\bar{C}\bar{\varepsilon}^{(k)} = \bar{\sigma}^{(k)}, \quad \bar{\sigma}^{(k)} = |\Omega|^{-1}\int_\Omega \sigma^{(k)} d\Omega, \quad \bar{\varepsilon}^{(k)} = |\Omega|^{-1}\int_\Omega \varepsilon^{(k)} d\Omega.$$

Assuming isotropy of the homogenized elasticity tensor, one loading is sufficient for getting elasticity constants. If $\xi = \xi_{vol} + \xi_{dev}$, is the decomposition of $\xi \in R^{6\times 6}_{sym}$ into the volumetric and deviatoric parts and $\|\cdot\|$ is the Frobenius norm, then the bulk and shear moduli can be determined as

$$K = \frac{1}{3}\,\|\bar{\sigma}_{vol}\| \,/\, \|\bar{\varepsilon}_{vol}\|, \quad G = \frac{1}{2}\,\|\bar{\sigma}_{dev}\| \,/\, \|\bar{\varepsilon}_{dev}\|\,.$$

For parameter identification, we assume that some local material properties are unknown, e.g. that the concrete matrix is described by unknown parameters $p = (K_c, G_c)$, where $K_c$ and $G_c$ are unknown bulk and shear parameters of the concrete. More generally, $\Omega$ can be split into subdomains with different unknown elastic moduli of concrete. Then the parameters are found by minimization of a proper objective function $J$ over a set of admissible parameters, see e.g. [7].

The construction of the objective function can be as follows

$$J(p) = \sum_k \left[ w_{1k} \left\| \bar{\varepsilon}^{(k)}(p) - \bar{\varepsilon}^{(k)}_{test} \right\|^2 + w_{2k} \left\| \bar{\sigma}^{(k)}(p) - \bar{\sigma}^{(k)}_{test} \right\|^2 \right],$$

where $\bar{\sigma}^{(k)}(p)$ and $\bar{\varepsilon}^{(k)}(p)$ are averaged stresses and strains computed by solving the boundary value problem in $\Omega$ with given microstructure, local material properties involving the parameters from $p$ and the loading $L^{(k)}$. This boundary value problem represents a physical test on the specimen $\Omega$. The test configuration is such that in the case of homogeneity of $\Omega$, the problem has a solution with unique and constant stress $\bar{\sigma}^{(k)}_{test}$ and strain $\bar{\varepsilon}^{(k)}_{test}$, which can be determined from measurements. The weights $w_{ik}$ can be determined by numerical experiments or simply set to be equal $w_{ik} = 1$.

The optimization is performed by a suitable method, we already successfully tested the Nelder-Mead and Gauss-Newton methods.

More details on the exploited homogenization and identification methods can be found in [3, 4].

## III. Additive Schwarz solver with two-level parallelization

A crucial component of the homogenization and identification procedures is the solver for boundary value problems of elasticity. We assume finite element discretization leading to algebraic systems of the type of $Au = b$ or $A(p)u(p) = b$, where later indicates dependence on some local material parameters. The system can be solved by the preconditioned conjugate gradient (PCG) method with one level additive Schwarz (AS) preconditioner $B_{AS1}$ and mostly its extended two-level version $B_{AS2}$,

$$B_{AS1} = \sum_{k=1}^{N} R_k^T \tilde{A}_k^{-1} R_k, \quad B_{AS2} = B_{AS1} + R_0^T \tilde{A}_0^{-1} R_0.$$

Here $R_k$ is a restriction defined by subdomain $\Omega_k$ or algebraically by overlapping decomposition of the solution vector $u \in R^n$, $\tilde{A}_k$ is an approximation to $A_k = R_k A R_k^T$. In our case $\tilde{A}_k$ is a displacement decomposition - incomplete factorization of $A_k$. The one level AS preconditioner is not scalable, the number of iterations increases with $N$, although this grow is a bit compensated by the fact that $\tilde{A}_k$ becomes a better approximation to $A_k$. It fits the algebraic form of the Schwarz methods if $R_0 \in R^{n_0 \times n}$ is a Boolean matrix, which defines aggregation of degrees of freedom, i.e. each row of $R_0$ defines one aggregate by unities in this row. On the other hand, each degree of freedom corresponds to just one aggregate, i.e. there is precisely one unity in each column of $R_0$. More details about this setting can be found e.g. in [2].

In the case of computing at a massively parallel computer like Salomon [8], it is possible to exploit hundreds of processors, which makes the local problems $A_k$ small even for large scale matrices $A$. It makes difficult to keep balance of times for solving the local problems $A_k$ and the coarse global one $A_0$. For this reason, parallel inner CG iterations for the solution of problem $A_0$ were suggested and the algorithm become with two levels of parallelization.

## IV. Numerical experiments

Our numerical experiments present five real samples of fiber-reinforced concrete, each of cubic shape and size 35 mm.

| Variant | Steel fibers [kg/m$^3$] | Volume Steel [%] | Volume Voids [%] |
|---|---|---|---|
| 0 | 0 | 0.00 | 1.55 |
| 2 | 50 | 0.92 | 1.22 |
| 3 | 100 | 1.82 | 0.75 |
| 4 | 150 | 2.57 | 0.71 |
| 5 | 200 | 2.11 | 1.83 |

*Table 1: Characteristics of REV for each sample of reinforced concrete. Variants differ in the volumes of steel fibers as well as voids. The size of fibers: length 6 mm, diameter 0.12 mm.*

Their microstructure is taken from industrial CT scanning performed at the CT lab of the Institute of Geonics. Digital

models arose from meshes of approx. 1400×1400×1400 voxels, which were further trimmed to 1000×1000×1000 voxels due to surface damage or irregular sides of the samples.

Consequent computational models use smaller representative volumes (REV) and standard linear tetrahedral finite elements. The size of each REV is 400×400×400 for homogenization experiments or 100×100×100 voxels for tests related to material identification, respectively. Accordingly the model leads to a (repeated) solution of the resulting linear system in size of about 193 millions or 3 millions degrees of freedom. Main characteristics of each REV are summarized in Tab. 1.

| Material | $E$ [GPa] | $\nu$ |
|---|---|---|
| concrete | 19 | 0.2 |
| steel | 200 | 0.3 |
| voids | 0.01 | 0.1 |

*Table 2: List of involved materials and their properties (Young's modulus E and Poisson's ratio ν).*

The properties of the materials involve in mathematical modelling are listed in Tab. 2. Voids (air bubbles in the microstructure) bring a kind of singularity caused by the finite elements weekly hanged in the void space. They are replaced with a very week elastic material. The convergence of the applied PCG method is then smoother and faster.

The arising large-scale systems of linear equations are processed by parallel solvers based on the PCG method, with stabilization in the singular case [10]. The computations are performed on SGI cluster Salomon [8] run by the IT4Innovations National Supercomputing Center in Ostrava. The cluster, currently on 55. place in Top500, consists of 24192 cores and 129 TB of memory in total and with the theoretical peak performance over 2 Pflop/s. The most of its compute nodes is equipped by two 12-core processors Intel Xeon E5-2680 v3 and 128 GB of memory.

Tab. 3 gives the results of numerical homogenization applying pure Dirichlet and pure Neumann boundary conditions (BC). The choice of BC sets a configuration of homogenization procedure, which simulates an appropriate laboratory test under uniaxial loading. Dirichlet BC prescribe some non-zero displacement on the top side in the direction of uniaxial loading, the other sides have zero normal displacements. Neumann BC enter opposite non-zero forces on the top and bottom sides in the direction of uniaxial loading, the other sides have zero normal forces. The use of pure Dirichlet and pure Neumann BC allows us to get upper and lower bounds for the upscaled elasticity tensor, see e.g. [3].

Due to irregular placement of steel fibers as well as voids

| **Dirichlet BC** | | | | | | |
|---|---|---|---|---|---|---|
| Variant | $E$ [GPa] | | | $\nu$ | | |
| | 18.365 | 18.370 | 18.407 | 0.199 | 0.199 | 0.199 |
| 0 | | 18.381 | | | 0.199 | |
| | 19.050 | 18.960 | 19.063 | 0.200 | 0.201 | 0.200 |
| 2 | | 19.024 | | | 0.200 | |
| | 20.015 | 19.621 | 19.768 | 0.200 | 0.202 | 0.201 |
| 3 | | 19.801 | | | 0.201 | |
| | 20.865 | 19.977 | 19.960 | 0.198 | 0.203 | 0.203 |
| 4 | | 20.267 | | | 0.201 | |
| | 19.345 | 19.508 | 19.715 | 0.202 | 0.202 | 0.201 |
| 5 | | 19.523 | | | 0.202 | |

| **Neumann BC** | | | | | | |
|---|---|---|---|---|---|---|
| Variant | $E$ [GPa] | | | $\nu$ | | |
| | 18.307 | 18.305 | 18.216 | 0.199 | 0.199 | 0.197 |
| 0 | | 18.276 | | | 0.198 | |
| | 18.692 | 18.822 | 18.798 | 0.197 | 0.199 | 0.199 |
| 2 | | 18.771 | | | 0.198 | |
| | 19.912 | 19.599 | 19.716 | 0.203 | 0.199 | 0.201 |
| 3 | | 19.742 | | | 0.201 | |
| | 20.613 | 19.948 | 19.435 | 0.204 | 0.199 | 0.195 |
| 4 | | 19.999 | | | 0.199 | |
| | 18.297 | 17.193 | 19.213 | 0.190 | 0.178 | 0.199 |
| 5 | | 18.234 | | | 0.189 | |

*Table 3: Results obtained by numerical homogenization applying Dirichlet and Neumann BC. Values of material parameters for different directions (X Y Z) of uniaxial loading and averaged (below).*

in the microstructure, the results documents the anisotrophy of tested material, when the values of material properties strongly vary for different directions of loading, e.g. the Young's modulus $E$ (the sample 4, Neumann BC) in Tab. 3 varies about more than 1 GPa. However as expected and consistent with theory, their averaged values follow the increase of volume of steel fibers in concrete.

The corresponding values for pure Dirichlet and pure Neumann BC give quite close bounds for real material properties. However we observe that these bounds grow away with the increasing volume of voids in the microstructure, moreover when the voids are closer to the border of the studied domain and pure Neumann BC are applied, see the values for the sample 5. Comparing with the others, the sample 5 contains also another abnormality. Although this sample should contain the most of steel fibers according to Tab. 1, the real volume of steels in REV is not the biggest. Moreover,

REV of this sample overcomes the others in the volume of the void space in its microstructure.

The previous tests were related to the direct problem denoting a computation of stiffness of the fiber reinforced concrete based on known material distribution and local material properties. The next numerical experiments describe one of the possible inverse problems, an identification of the material properties (Young's modulus $E$ and Poisson ratio $\nu$) of the concrete matrix from known material distribution, elastic properties of fibers and response of the sample (REV) to uniaxial or triaxial loading tests. This inverse problem exploits the objective function (the cost functional) $J(p)$, $p = (E, \nu)$, $w_{1k} = w_{2k} = 1$, introduced in the section II. For more details see [3].

| **Dirichlet BC** | | | |
|---|---|---|---|
| Variant | Steps | $E$ [GPa] | $\nu$ |
| 0 | 135 | 19.020 | 0.199 |
| 2 | 141 | 19.000 | 0.200 |
| 3 | 141 | 19.005 | 0.200 |
| 4 | 141 | 19.029 | 0.200 |
| 5 | 141 | 19.007 | 0.200 |

| **Neumann–Dirichlet BC** | | | |
|---|---|---|---|
| Variant | Steps | $E$ [GPa] | $\nu$ |
| 0 | 138 | 18.996 | 0.200 |
| 2 | 135 | 19.004 | 0.200 |
| 3 | 135 | 19.006 | 0.200 |
| 4 | 162 | 19.034 | 0.200 |
| 5 | 129 | 19.007 | 0.200 |

*Table 4: Results of material identification applying Dirichlet and Neumann-Dirichlet BC. The number of transformation steps of the applied Nelder-Mead method and the identified averaged material properties of the concrete matrix for each REV.*

The optimization is performed by the non-gradient Nelder-Mead (NM) method with starting values ($E$, $\nu$) provided by three pairs (17.000, 0.26), (21.000, 0.17), (18.000, 0.23). In each step of the NM method, three direct problems (three computation of local stresses and strains), corresponding to simulation of uniaxial loading tests for each direction X, Y and Z, are solved. Dirichlet BC describe the same loading as in case of homogenization tests. Neumann-Dirichlet BC enter a combination of pure Dirichlet and pure Neumann BC introduced earlier. It means the prescribed non-zero displacement on the top side in the direction of loading, zero displacement on the bottom side in the direction of loading and zero normal forces on the other sides. The NM iterations are stopped if the decrease of the cost functional and differences in the identified parameters are sufficiently small.

The numbers of transformation steps performed by the NM optimizaton procedure and the averaged values of the identified material properties are summarized in Tab. 4. Dirichlet BC on the whole sample boundary are used for comparison purposes. They are applicable if the loading response is computed artificially. The obtained results show a good accordance with the values for the concrete matrix presented in Tab. 2. Considering the number of NM steps and a need to repeat the FEM calculation several times in each step, the results document also a substantially increased requirements on the computational power of the used computer.

## V. Tuning of parallel solvers

Nowadays powerful parallel computers for HPC have hundreads or thousands of cores. Therefore we decided to reimplement our original parallel solver for large-scale systems of linear equations arising from 3D boundary problems of elasticity. The solver dates back to the times of Beowulf type clusters and small multiprocessors with up to 20 processors.

The original solver is based on the PCG method, uses the one-directional domain decomposition for parallelization of iterative process as well as the construction of efficient one-level and two-level AS preconditioners (AS1, AS2), see their definition through $B_{AS1}$ and $B_{AS2}$ in III. Parallel processes communicate through message passing (MPI standard).


*Figure 1: Traces of one PCG iteration processing 4 subdomains. From above, records for the original solver with AS1 and AS2, and new solver with AS1 only. States of parallel processes: work (blue), wait or idle (red).*

Fig. 1 shows traces of the runs of parallel solvers produced by the Intel Trace Analyzer. The implementation of the

original solver follows the master-slave design, when the first process (from above) is the master, almost idle, just controlling the iterative process and computing two global scalar products. Each of the four slave processes (below the master) works on its portion of data, especially during the dominating operations matrix by vector multiplication (MXV) and preconditioning (PREC).

The second trace adds a coarse grid computation to AS2. This computation is performed by a separate process, idle for more than a half of the iteration execution time. Nevertheless this process is very important because a coarse grid computation strongly improves the efficiency of the preconditioner and speeds up the convergence of the PCG iterations.

The third trace documents a run of the new version of the parallel solver, surpassing the original one in the execution time and a better utilization of processes. New solver works internally with data in double precision and dynamic allocation of memory, uses a modified domain decomposition (with an overlapping of subdomains) leading to a better load balancing of processes, has optimized (mainly global) communication of processes and also calculations in loops (during MXV and PREC operations). The new solver abandons master-slave design, the negligible amount of work performed by the master process was taken over by the other processes.

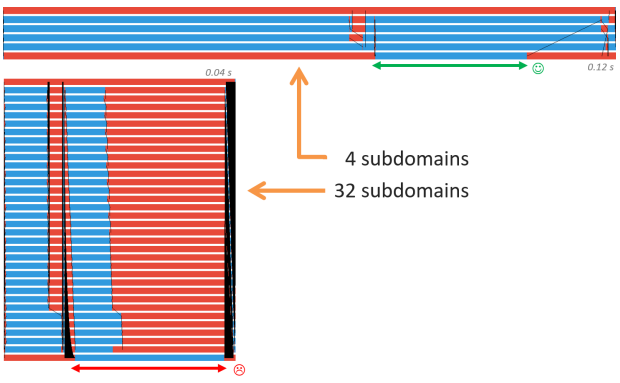


*Figure 2: A coarse grid computation bottleneck in the original solver. Traces of one PCG iteration processing 4 and 32 subdomains.*

The next step in the parallel solver optimization is indicated by Fig. 2. With the increase of processes, the execution time of the most demanding MXV and PREC operations performed by worker processes scales down correspondingly, whilst the execution time of a coarse grid computation stays constant. In the example shown in Fig. 2, the described effect limits the possible speed-up of the solver only to 3, instead of expected 8, which corresponds to the increase of the number of processes.

Such a negative effect can be eliminated by a coarse grid parallelization in a hybrid way, when all processes do not perform the same calculations. On hundreads of computing elements (processors or cores), such hybrid parallelization includes the most of processes solving the subproblems corresponding to subdomains and only a few (units or tens) of processes performing coarse grid computations in parallel. It should not substantially decrease convergence properties of the applied AS2 preconditioner, but dramatically increase the efficiency of the resulting PCG iterations. However, the described hybrid paralellization can bring difficulties how to treat optimal load balancing of processes.

## VI. Conclusions

The paper demonstrates the need for high performance computing by focusing on one engineering application - investigation of the fiber reinforced concrete. The primary analysis solves a microscale problem for homogenization within the range of linear material behaviour. This basic problem can be modified (extended) in several directions and any of them substantially increases the computational demands. One extension, roughly described in this abstract, is the solution of the inverse problem of identification of the local material parameters or some level of debonding of the matrix and fibers. This problem is solved by the optimization methods which require repeated solution of the basic problem. The increase in computational demands can be about hundred times. Another extension is based not only on the solution of selected and scanned samples of the concrete, but also on the stochastic generation of a set of such samples and evaluation of the mean properties by Monte Carlo or multi-level Monte Carlo methods, see e.g. [9]. The last extension is to consider the strengths and non-linear post peak behaviour, which involves the usage of damage mechanics techniques, see e.g. [5] and the references therein.

**Acknowledgement:** The work is supported by COST Action IC1305 project Network for Sustainable Ultrascale Computing and a bilateral project of collaboration between the Institute of Geonics CAS and IICT BAS. Further support is through the projects LD15105 Ultrascale computing in geosciences and LQ1602 IT4Innovations excellence in science supported by the Ministry of Education, Youth and Sports of the Czech Republic.

## References

[1] R. Blaheta, A. Kolcun, O. Jakl, K. Souček, J. Starý and I. Georgiev: *HPC in Computational Micromechanics of Composite Materials.* NESUS workshop, Cracow, Poland, 2015.

[2] R. Blaheta, O. Jakl, R. Kohut and J. Starý: *GEM - A Platform for Advanced Mathematical Geosimulations.* In: R. Wyrzykowski et al. (eds.): PPAM 2009, Part I, LNCS 6067, 2010, pp. 266–275.

[3] R. Blaheta, R. Kohut, A. Kolcun, K. Souček, L. Staš and L. Vavro: *Digital image based numerical micromechanics of geocomposites with application to chemical grouting.* International Journal of Rock Mechanics and Mining Sciences. Vol. 77 (2015), pp. 77-88.

[4] R. Blaheta, R. Kohut and J. Starý: *Computational and reliability aspects of micro-geomechanics.* In: Oka, Murakami, Uzuoka and Kimoto (eds.): Computer Methods and Recent Advances in Geomechanics, Taylor & Francis Group, London, 2015.

[5] M.A. Hickman and P.K. Basu: *Stochastic Multiscale Characterization of Short-Fiber Reinforced Composites.* Technische Mechanik, 36, Vol. 1-2 (2016), pp. 13–31.

[6] X. Guan, X. Liu, X. Jia, Y. Yuan, J. Cui and H.A. Mang: *A stochastic multiscale model for predicting mechanical properties of fiber reinforced concrete.* International Journal of Solids and Structures, Vol. 56–57 (2015), pp. 280–289.

[7] J. Haslinger, R. Blaheta and R. Hrtus: *Identification problems with given material interfaces.* Journal of Computational and Applied Mathematics, early view June 2016.

[8] *Salomon Cluster Documentation*, https://docs.it4i.cz/salomon

[9] R. Blaheta, S. Domesová and M. Béreš: *A study of stochastic FEM method for porous media flow problem.* Proceedings of PhD workshop, Institute of Geonics CAS, December 2015.

[10] R. Blaheta, O. Jakl, J. Starý and E. Turan: *Parallel solvers for numerical upscaling.* In: PARA 2012, LNCS 7782, Springer-Verlag, 2013, pp. 375–386.